ORIGINAL PAPER

Electrochemical, theoretical, and morphological studies of antioxidant fullerosteroids

Mira Bjelaković · Tatjana Kop · Rada Baošić · Mario Zlatović · Andrijana Žekić · Veselin Maslak · Dragana Milić

Abstract Four fullerosteroidal conjugates, previously confirmed to express two- to threefold better antioxidant activity in vitro than C_{60}, were subjected to additional studies, including electrochemical, theoretical, and morphological examination. All tested compounds underwent reversible, diffusion-controlled reductions. A notable influence of the solvent properties on the reduction potential, the level of aggregation, and the lowest unoccupied molecular orbital (LUMO) energy was observed. Theoretical calculations indicated that the energy gain obtained by an intermediate formation, together with compounds' polarizability, polarity, and lipophilicity contributed to the radical quenching capacity. Very large supramolecular aggregates of all fullerosteroidal esters with no hierarchical arrangement were observed in precipitated samples, while solvent induced self-assembling led to round nanoplates, which further arranged to flower-shaped hierarchically ordered architectures or uniformly distributed discoid particles. As in electrochemical studies, fine tuning of the aggregation level was achieved by the solvent.

R. Baošić · M. Zlatović · V. Maslak · D. Milić (✉)
Faculty of Chemistry, University of Belgrade, Belgrade, Serbia
e-mail: dmilic@chem.bg.ac.rs

M. Bjelaković · T. Kop
Center for Chemistry, ICTM University of Belgrade,
Belgrade, Serbia

A. Žekić
Faculty of Physics, University of Belgrade, Belgrade, Serbia

Introduction

Among many benefits, the progress of material science to the nanoscale allowed the possibility to engineer biologically active molecular devices and to design targeted drug delivery. The observation that nanoparticles, especially fullerenes, can act as a radical scavengers opened a broad spectrum of investigation in their potential application in biological systems. Their limited bioavailability, resulted from the complete lack of solubility in water and quite low solubility in almost all organic solvents can be prevailed by assisted solubilization or by covalent modification. Besides increasing of solubility, the later method could also afford compounds with significantly changed properties, thus expanding the fullerene application.

The protective action of C_{60} derivatives, particularly superoxide radical quenching activity was extensively examined. Widely studied tris-malonyl trimethanofullerene expressed activity smaller than corresponding natural enzymes, but at the range of several metal-containing superoxide dismutase (SOD)-mimetics [1]. Also, an enhancement of the antioxidant capacity of polyamines was observed after the formation of corresponding *N*-substituted fulleropyrrolidines [2]. Structure–function studies on methanofullerenes containing carboxylic groups indicated an influence of several parameters on the antioxidant properties, such as the redox behavior, number of the introduced addends, charge, size, shape, hydrophobicity, dipole moment, and the molecular architecture. According to our knowledge, similar detailed examination in the family of fulleropyrrolidines was not performed so far. It has been shown that high catalytic SOD activity of mono-methanofullerene derivatives and their first reduction potential were directly proportional. Compounds with higher first reduction potential were more susceptible to

reduction and quenched the superoxide radical easier, acting at lower concentration and with higher rate constant [3]. More extensive investigation, performed on the large series of variously functionalized methanofullerenes revealed that an increased disruption of the fullerene π-system caused a decrease in antioxidant activity, but also indicated that multiple independent factors other than redox properties could play major role. In this context, in determining the antioxidant efficiency the shape, size, charge and hydrophobicity of each fullerene derivative should be considered [4], as well as its dipole moment and lipophilicity/hydrophilicity balance [5]. Theoretical calculations of energetic changes during electron transfer from superoxide radical to methanofullerenic acids revealed that experimentally observed direct proportionality of SOD activity and the first reduction potential was a consequence of decreasing energy difference between the highest occupied and the lowest unoccupied molecular orbital (HOMO and LUMO) of reacting species [6].

Beside the chemical structure, the susceptibility of carbon nanoparticles to assemble and form aggregates appeared to be important in determining their biological activity. For example, the pro-oxidant activity of fullerene was decreased in more compact aggregates due to facilitated triplet–triplet annihilation resulted from close proximity of individual molecules [7]. Although the quantum yield of fullerol is lower by an order of magnitude in comparison to C_{60}, the hydroxylated derivative expressed higher photoinduced pro-oxidant capacity than pristine fullerene. It was considered that the formation of smaller and less compact aggregates in which the self-annihilating triplet–triplet interactions were reduced also increased an effective availability to approaching oxygen, and consequently facilitated production of reactive oxygen species (ROS) [8]. As a consequence, fabricating and controlling molecular architectures with desired structures and properties remains a constant challenge in chemistry and material science.

A pronounced solvophobicity of fullerene and its derivatives as well as tuning intermolecular interactions by sample preparation under different conditions enabled formation diverse supramolecular self-assembled aggregates. Various shapes of amphiphilic fullerene-based functional nanostructured materials, including wires [9], rods [10], tubes [11], sheets [12], spheres [13], fibers [14], or vesicles [15] are formed by solvent or temperature control. Contrary to the multitude of fullerene derivatives that have so far been published, only a few examples of fullerenes bearing different steroid moieties have been reported [16–23]. Such systems have all important characteristics typical for self-assembling process, primarily a large hydrophobic surface area that can provide an efficient

platform for the formation of highly organized structures. Nevertheless, to the best of our knowledge studies of self-organization abilities of fullerosteroids have not been reported so far.

In our previous work [16], we showed the synthesis of fullerosteroidal esters that expressed higher in vitro antioxidant activity than the parent fullerene. In addition, all of them fluoresced stronger with respect to pristine C_{60}, thus representing good potential irradiation-assisted pro-oxidants, too. Therefore, it could be expected that further investigation of their properties, primarily the electrochemical and the aggregation ones, might contribute to the better understanding of observed activity.

Here, we present an additional study of four steroid-conjugated fulleropyrrolidinic esters connected by a short alkyl linker (Fig. 1): 4-(3′,4′[1,9](C_{60}-I_h)[5,6]fulleropyrrolidin)-1-yl-butanoic acid 17-acetyl-10,13-dimethyl-2,3,4,7,8,-9,10,11,12,13,14,15,16,17-tetradecahydro-1H-cyclopenta[a]-phenanthren-3-yl ester (1), 4-(3′,4′[1,9](C_{60}-I_h)[5,6]fulleropyrrolidin)-1-yl-butanoic acid 17-acetyl-10,13-dimethyl-2,3,4,7,8,9,10,11,12,13,14,15,16,17-tetradecahydro-1H-20-oxa-cyclopropa[16,17]cyclopenta[a]phenanthren-3-yl ester (2), 4-(3′,4′[1,9](C_{60}-I_h)[5,6]fulleropyrrolidin)-1-yl-butanoic acid 17-hydroxy-13-methyl-7,8,9,11,12,13,14,15,16,17-decahydro-6H-cyclopenta[a]phenanthren-3-yl ester (3), and 4-(3′,4′[1,9](C_{60}-I_h)[5,6]fulleropyrrolidin)-1-yl-butanoic acid 17-ethynyl-17-hydroxy-13-methyl-7,8,9,11,12,13,14,15,16,17-decahydro-6H-cyclopenta[a]phenanthren-3-yl ester (4). In order to better understand their already observed radical scavenging capacity and compounds properties as a whole, electrochemical and morphological investigations, supported by molecular modeling were performed.
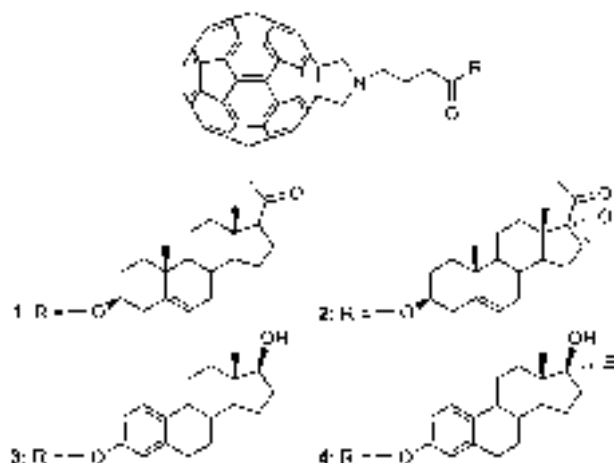

Fig. 1 Structures of investigated fullerosteroidal esters

Results and discussion

Electrochemistry

The electrochemical properties of fullerosteroidal esters **1**–**4** were investigated by cyclic voltammetry (CV) in solution using *N,N*-dimethylformamide (DMF) and dichloromethane (DCM) as the solvents. Selected CV curves of studied compounds recorded in DMF/tetrabutylammonium perchlorate (TBAP) at 298 K and the scan rate of 0.3 V/s are given in Fig. 2, while representative voltammograms of compound **1** in different solvents at 298 K and the scan rate of 0.1 V/s are presented in Fig. 3. Observed half-wave reduction potentials of compounds **1**–**4**, and corresponding LUMO energy levels calculated from the CV data as well as those obtained by molecular modeling are collected in Table 1.

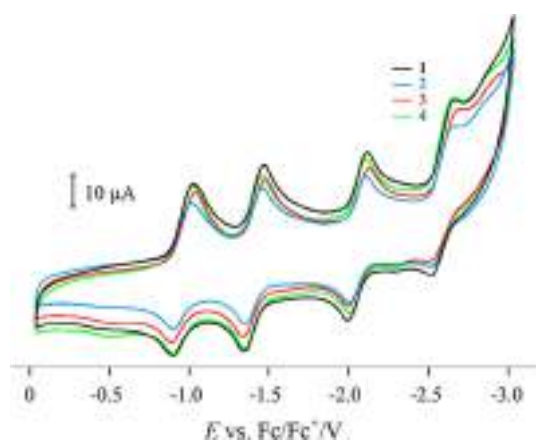The studied compounds have quite similar molecular structures, so their electronic properties, in particular

Fig. 2 Cyclic voltammograms of 1-mM solution of **1**–**4** in DMF containing 0.1-M TBAP at 298 K and the scan rate of 0.3 V/s
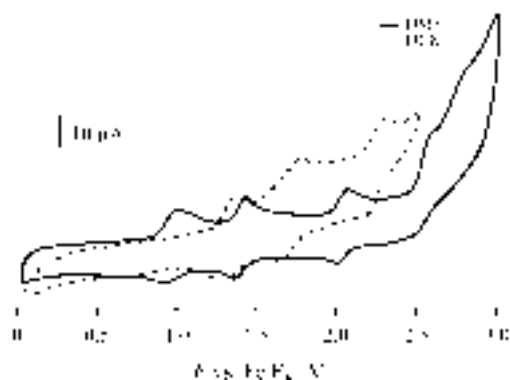

Fig. 3 Cyclic voltammograms of 1-mM solution of **1** in DMF (*solid*) and DCM (*dashed*) containing 0.1-M TBAP at 298 K and the scan rate of 0.1 V/s

frontier orbital energy levels should also be very similar. As expected, all four compounds gave almost identical CV curves (Fig. 2) typical for fulleropyrrolidines. A notable influence of the solvent on the first and the second half-wave potentials was observed (Table 1; Fig. 3). In the cathodic scan in a DCM solution, three regularly separated reversible one-electron reductions were observed in the accessible potential window, all attributable to the fulleropyrrolidinic subunit. Corresponding half-wave potentials ($E_{1/2}$) were located at ca. −1.1, −1.5, and −2.0 V (first to third), respectively. The CV curves relative to a DMF solution of fullerosteroids **1**–**4** display a series of four well defined, successive reversible one-electron reductions of fulleropyrrolidine moiety, located at ca. −1.0, −1.4, −2.0, and −2.6 V ($E_{1/2}$ values, first to fourth), respectively. All half-wave potentials in both solvents are ca. 200 mV negatively shifted with respect to pristine C_{60} due to partially lost delocalization of π-electronic system over carbon sphere upon [3 + 2]-cycloaddition (Table 1). The first two reductions of all four compounds proceeded easier in DMF and corresponding half-wave potentials were ca. 100 mV positively shifted with respect to DCM. The third reduction potentials remained independent on the solvent used.

The reduction potentials of fullerenes strongly depend on the solvent, mainly on its electron-accepting and donating capacity [24, 25] described with Dimroth–Reichardt parameter (E_T^N) and Gutmann donor number (*DN*), respectively. The corresponding parameters of used solvents are [24] $E_T^N(30)$: 0.309 (DCM); 0.404 (DMF) and DN: 0.0 (DCM); 26.6 (DMF). As can be seen both values are higher for DMF indicating that facilitated reduction is a consequence of the stabilization of generated fullerosteroidal anions by the solvent electron-accepting ability, as well as the compounds reduced aggregation by the solvent electron-donating capacity.

The effect of the scan rate was investigated by performing CV experiments at 0.1, 0.3, 0.5, and 1 V/s in DMF and 0.05, 0.1, 0.2, and 0.5 V/s in DCM. The values of the half-wave potentials were found to be independent on the scan rate, as was expected for a reversible system. In addition, all anodic as well as cathodic peak currents in both solvents varied linearly with the square root of the scan rate ($v^{1/2}$), indicating diffusion-controlled reductions. Also, the products of all four reductions are stable on the cyclic voltammetric time scale since neither additional peaks during five consecutive scans, nor any change in the NMR spectra of quantitatively recovered compounds was not detected.

The CV measurements allow the possibility to determine the diffusion coefficient (*D*) of the examined compound, and further its hydrodynamic radius. In such a way, the potential supramolecular interactions, primarily self-aggregation under applied conditions, can be studied

Table 1 Half-wave reduction potentials and the LUMO energy levels of fullerosteroids **1–4** in DMF/DCM

Compound	$E_{1/2}$/V				LUMO/eV	
	I	II	III	IV	CV[a]	MM[b]
1	−0.98/−1.12	−1.40/−1.52	−2.05/−2.06	−2.55/−	−4.38/−4.73	−3.82
2	−0.96/−1.14	−1.40/−1.53	−2.05/−2.06	−2.58/−	−4.36/−4.77	−3.90
3	−0.96/−1.14	−1.40/−1.53	−2.05/−2.05	−2.59/−	−4.36/−4.77	−3.65
4	−0.96/−1.11	−1.40/−1.49	−2.05/−2.01	−2.58/−	−4.36/−4.72	−3.65
C_{60}[c]	−0.77/−0.95	−1.25/−1.39	−1.84/−1.84	−2.38/−	−4.17/−4.56	−3.49

Half-wave reduction potentials vs. Fc/Fc$^+$ (0.53/0.32 V vs. Ag/Ag$^+$ in DMF/DCM)

[a] Calculated from the CV data

[b] Obtained by theoretical calculations

[c] Half-wave reduction potentials were taken from Ref. [24] and recalculated according to the Fc/Fc$^+$ value

more in detail. Translation mobility of the molecules in continuous incompressible fluids, determined by D, depends on the medium viscosity, solvent–particle interactions, as well as of the size and the shape of a molecule. For spherical particles it can be expressed by Stokes–Einstein relation:

$$D = k_B T / 6\eta r_s \qquad (1)$$

where k_B represents Boltzmann constant, T temperature, η the dynamic viscosity of the solvent (0.410 and 0.802 mPa s for DCM and DMF, respectively [24]), and r_s Stokes (hydrodynamic) radius. The diffusion coefficients of fullerosteroids **1–4** were calculated from the slope of the plot of the cathodic peak current vs. $v^{1/2}$ using Randles–Sevcik equation:

$$i_p = \left[D^{1/2} (2.69 \times 10^5) n^{3/2} Ac \right] v^{1/2} \qquad (2)$$

where i_p represents peak current, D diffusion coefficient, n the number of electrons transferred in the half reaction for the redox couple, A the electrode area, c concentration, and v scan rate. Including obtained values into Stokes–Einstein equation (1) afforded radii of solvated charged particles, given in Table 2. Under applied conditions in DMF fullerosteroidal anions of all tested compounds were detected as particles of ca. 3 nm in diameter, indicating the presence of individual molecules solvated by monomolecular layer of the solvent. On the other hand, in DCM which has no electron-donating capacity, compound's aggregation was not suppressed by the solvent and significantly larger particles were observed. Detected radii were four- to fivefolds bigger than calculated radius of individual compound increased by monomolecular solvent layer. The estrone-based fullerosteroids **1** and **2** formed particles of ca. 8 nm in diameter, while from pregnenolone-derived compounds **3** and **4** even larger aggregates of 10 nm in diameter were built.

Table 2 Diffusion coefficients D, hydrodynamic radii r_s of C_{60} and fullerosteroids **1–4** in DMF/DCM containing 0.1-M TBAP and their MM-calculated radii r_{MM}

Compound	$D \times 10^{-10}$/m^2/s	r_s/nm	r_{MM}/nm
1	1.78/1.02	1.53/5.20	0.83
2	1.68/1.00	1.62/5.32	0.83
3	1.97/1.35	1.38/3.94	0.81
4	1.87/1.32	1.45/4.02	0.82
C_{60}	–/4.4 [24]	–/1.11	0.68

Solvent radius/nm, calculated from the molecular weight and density of the solvent: 0.31 (DMF); 0.29 (DCM)

The CV is often used to calculate the energy levels of frontier orbitals although obtained data are only fairly comparable since the redox potentials are measured in solution, while orbital energies are scaled in vacuum. In this work, the LUMO energies have been additionally determined by theoretical calculations in vacuum, and afforded results were used only for relative comparison of compounds. Following the IUPAC procedure [26], the electrode potentials in non-aqueous solvents were measured against the potential of Fc/Fc$^+$ redox couple. In order to estimate the LUMO energy level of fullerosteroids **1–4**, the value of internal standard was evaluated against reference electrode and was found to be 0.53 V and 0.32 V vs. Ag/Ag$^+$ in DMF and DCM, respectively. Using the literature data of 0.29 V for the conversion of potentials measured vs. Ag/Ag$^+$ electrode to SCE [27] and 0.24 V for the potential of SCE vs. normal hydrogen electrode (NHE), experimentally observed reduction half-potentials of Fc/Fc$^+$ were recalculated to 1.06 and 0.85 V vs. NHE in DMF and DCM, respectively. There are several values that correlate the potential of NHE reference electrode to Fermi energy scale (the vacuum level), varying from −4.4 to −4.85 eV [28]. Setting the NHE vs. the vacuum level to

−4.46 eV [29], the LUMO level in the corresponding solvent was calculated from the formula:

$$E_{LUMO} = -4.46 + \left(E_{1/2} Fc/Fc^+ vs.\ NHE\ + E_{1/2}^{redI} \right)$$

where $E_{1/2}^{redI}$ represents the half-wave potential of the first reduction step.

Obtained LUMO energies of all four studied fullerosteroids were similar within the same solvent and appeared in a narrow range of −(4.36–4.38) eV in DMF and −(4.72–4.77) eV in DCM. Also their LUMO levels were ca. 200 meV more negative than the LUMO level of C_{60}. On the other hand, a significant variation in the LUMO energy levels of individual compounds of ca. 400 meV was observed in different solvents (twice higher than the difference caused by the π-conjugation disruption) with stronger stabilization by the solvent with higher electron-donating as well as electron-accepting capacity, i.e., DMF. For example, the LUMO energy level of compound **2** was located at −4.36 eV in DMF, whereas in DCM the value of −4.77 eV was achieved. Obtained results clearly showed the importance of the solvent selection in potential electrochemical modifications of fullerene and its derivatives, as well as the influence of an environment on redox processes.

Electrochemical properties vs. antioxidant activity

The literature data indicate that positive shifting of the first reduction potential of the fullerene derivatives induces the increase of their antioxidant activity [3]. Based on that, lower activity of fullerosteroids with respect to parent fullerene could be expected since their first reduction potentials were ca. 200 mV negatively shifted (Table 1). However, our previous results [16] showed that fullerosteroids **1–4** expressed two- to threefold stronger radical quenching than C_{60}. In addition, besides the redox properties, a mutual influence of the charge, shape, size and hydrophobicity on the antioxidant activity should be taken into consideration as well [4]. Furthermore, such activity was found to be related to the dipole moment too [5]. In order to determine parameters other than redox properties and their possible influence on the radical quenching capacity of fullerosteroids, all compounds were subjected to MM calculations.

Molecular modeling

In order to examine the electronic properties of four investigated fullerosteroidal esters more in detail and to understand better their antioxidant activity, the molecular geometries and electron density distribution were simulated by conformational search and single-point DFT

B3LYP quantum mechanical calculations, respectively. The most stable conformations of compounds **1–4**, distribution of their frontier orbitals, and corresponding electrostatic potential maps were depicted in Figs. 4, 5, and 6, respectively, while the values of the selected descriptors and properties are given in Table 3.

The conformation with the steroidal subunit bended towards fullerene sphere was found to be the most stable for all compounds (Fig. 4), indicating the importance of hydrophobic interactions in the polar environment. The center-to-center distances between steroidal and fullerene moieties were found to be 0.74–0.95 nm, where the midpoint of the steroidal C(7)–C(8) bond (the B/C rings conjunction) was chosen as the steroidal centre. Observed distances in the aromatic steroidal fulleroesters **3** and **4** were slightly shorter than in pregnenolone-derived conjugates **1** and **2** suggesting an existence of the π–π stacking interactions (Table 3). The distance of 0.36 nm between the steroidal aromatic A-ring and the nearest fullerene ring confirmed the presence of these interactions. Looking into the spatial distribution of the frontier orbitals shown in Fig. 5, it can be seen that in all cases the electron-accepting region, responsible for free radical quenching activity and determined by the presence of LUMOs, was localized on the fullerene core.

The possibility of eventual electrostatic interactions within the molecule as well as with solution/other solutes was investigated by calculation of their molecular electrostatic potentials map. The covalent modification of fullerene sphere induced the change in the electrostatic potential distribution (Fig. 6; Table 3). In general, small charge separation was observed in all compounds. The negative potential, presented by red color, was mainly associated with the oxygen atoms belonging to carbonyl, oxo, epoxy, and hydroxyl functions, while positive regions marked by blue color were located at the pyrrolidine ring and acidic hydrogen belonging to hydroxyl groups. The main part of the steroidal subunit as well as the whole carbon sphere remained with no charge separation (green), therefore the favorable interactions with non-polar environment such as the organic solvents and/or lipid membrane could be expected. Also, total solvent accessible (SA) volume and the corresponding surface area (SASA) increased by the fullerene functionalization (Table 3, entries 3 and 4). The participation of the hydrophobic component (FOSA) was significantly increased (ca. 50 % of the SASA) while the contribution of the hydrophilic components (FISA) was also observed, but in lower degree (less than 10 % of the SASA). Although fullerene-steroid conjugation produced relatively weak charge separation dipolar structures with dipole moment of ca. 6–8 D were formed, and in all four investigated compounds notably enlarged polarizability was observed (by 60–80 % with

Fig. 4 The most stable
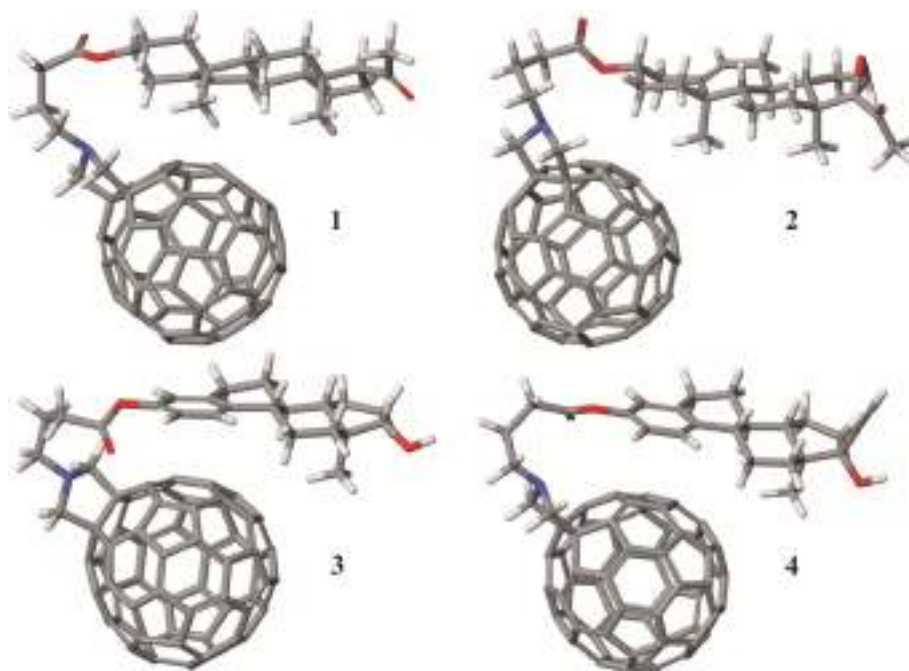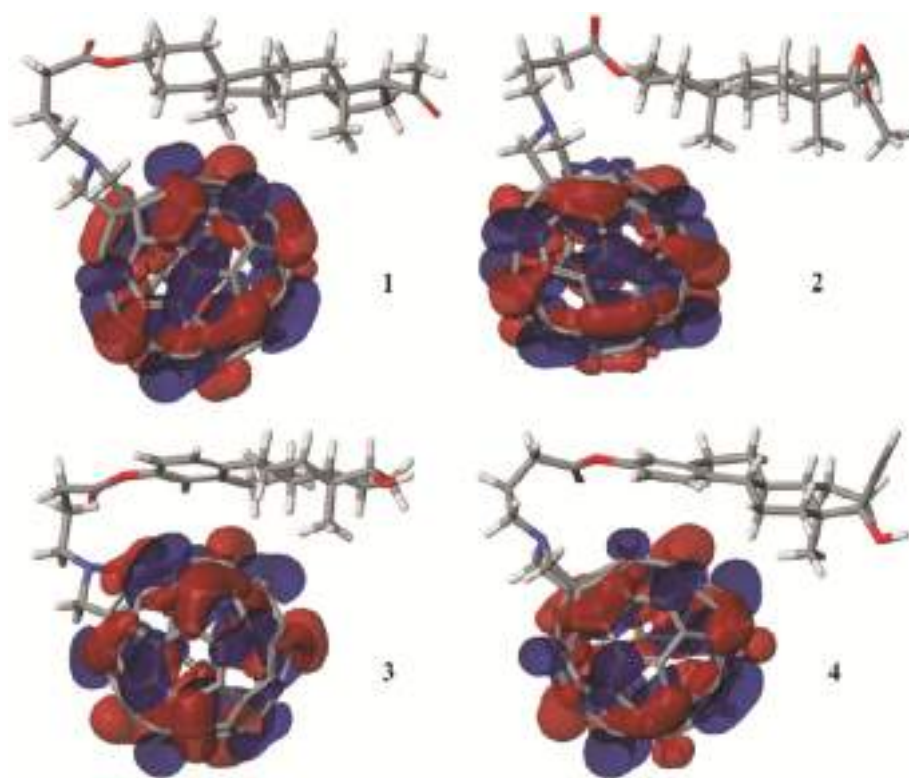conformations of fullerosteroids
1–4

Fig. 5 Molecular orbital spatial
orientation for the LUMO
energy levels of compounds **1–4**

respect to C_{60}). In addition, the covalent modifications of the fullerene sphere changed the ability of hydrogen bond (HB) formatting. The fullero-pregnenolone derivatives **1** and **2** showed moderate HB-accepting capacity, while their HB-donating ability remained unchanged in comparison to C_{60}. On the other hand, estradiol-derived fullero

compounds **3** and **4** could participate in HB formatting as acceptors, but also as weak donors (Table 3, entries 10 and 11). Introduction of the steroidal subunit led to considerably increased lipophilicity of carbon clusters augmenting the log P values by 2–3 units (Table 3 entry 12), once more indicating facilitated interactions with non-polar media.

Fig. 6 Molecular electrostatic potential maps for the most stable conformations of compounds **1–4** (conformations determined by conformational search, electrostatic potential is depicted by mapping it on electron density)
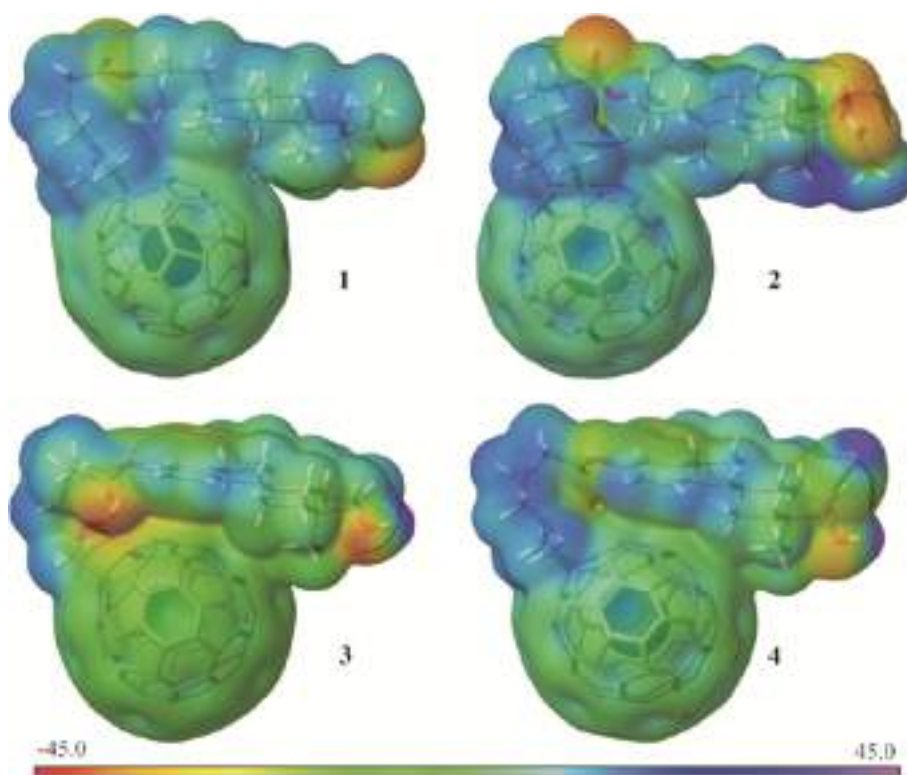

Table 3 Selected calculated properties and descriptors of C_{60} and fullerosteroids **1–4**

Entry	Property/descriptor	C_{60}	**1**	**2**	**3**	**4**
1	ED_{50}/μM[a]	64	28	28	20	27
2	Center-to-center distance/nm	–	0.87	0.95	0.74	0.74
3	SA volume/(Å^3)[b]	1,298	2,372	2,423	2,228	2,344
4	SASA/(Å^2)[c]	589	981	1,019	914	963
5	FOSA/(Å^2)[d] (% of SASA)	0 (0)	478 (49)	476 (47)	402 (44)	424 (44)
6	FISA/(Å^2)[e] (% of SASA)	0 (0)	83 (8)	81 (8)	60 (6)	55 (6)
7	PISA/(Å^2)[f] (% of SASA)	589 (100)	420 (43)	462 (45)	452 (50)	484 (50)
8	Dipole/D[g]	0	7.22	6.06	6.96	7.60
9	QP polrz/(Å^3)[h]	51.43	88.94	91.37	83.50	87.80
10	acceptHB[i]	0	6	8	6.2	5.2
11	donorHB[j]	0	0	0	1	1.5
12	QP log P o/w[k]	7.79	11.24	10.66	10.40	11.54

[a] Experimentally obtained results of the antioxidant activity [16] are given for comparison

[b] Total solvent accessible volume using a probe with a 1.4 Å radius

[c] Total solvent accessible surface area using a probe with a 1.4 Å radius

[d] Hydrophobic component of the SASA

[e] Hydrophilic component of the SASA

[f] π-Component of the SASA

[g] Computed dipole moment

[h] Predicted polarizability

[i] Estimated number of HB that would be accepted by the solute from H_2O in an aq. solution

[j] Estimated number of HB that would be donated by the solute to H_2O in an aq. solution

[k] Predicted octanol/water partition coefficient (lipophilicity)

Alterations of the solvent–solute interactions together with dipole formation, increased affinity to HB formation and enhanced lipophilicity could explain experimentally observed improved solubility of fullerosteroids with respect to pristine C_{60}. Thus, all four investigated compounds are easily soluble in chloroform (15 mg/cm^3; C_{60} 0.16 mg/cm^3 [30]) and in solvent mixture CHCl$_3$/CS$_2$/MeOH (1/1/1 volume ratios; 5 mg/cm^3), while in more polar CHCl$_3$/MeOH (4/1 v/v) mixture the moderate solubility of 2 mg/cm^3 was reached.

Obtained results pointed out that some molecular properties and descriptors could contribute to the previously observed in vitro free radical quenching activity [16]. Thus, calculation the Pearson correlation coefficient (PCC) [31] showed strong positive association of the antioxidant activity with polarizability, polarity, and the solvent accessible surface area (Table 4). Good correlation with lipophilicity was also observed, while very low linear associations with the LUMO level, as well as the half-wave reduction potentials were found.

Usually, the radical quenching activity of fullerene derivatives decreases with lowering their first reduction potential due to the disruption of the fullerene π-system and consequent reduced affinity to accept an electron. On the other hand, since an electron transfer could involve the interaction of donating and accepting species, the energy levels of their frontier orbitals should also be taken into consideration. According to the equation reported by Sales and Klopman the closer in energy the two orbitals are, the more significant the energy gain will be achieved by their interactions. Therefore, the comparison of the frontier orbital energies of donating and accepting compounds seemed reasonable.

The single occupied molecular orbital (SOMO) energy level of peroxylinoleic radical (LOO$^{\bullet}$) used in our previous in vitro experiments was found to be −6.22 eV [32]. Comparing the SOMO–LUMO differences, where the LUMO values were taken from CV-derived calculations, showed that in both investigated solvents frontier orbitals of fullero derivatives were for ca. 200 meV (∼19 kJ/mol) closer to donating radical species with respect to non-

Table 4 The correlation of the antioxidant activity with molecular descriptors/properties expressed by the PCC

Descriptor/property	PCC
Polarizability	0.93
Polarity	0.90
SASA	0.89
Log P o/w	0.63
LUMO (MM)	−0.24
$E_{1/2}$ (I)	−0.39

Table 5 SOMO$_{LCOO\bullet}$-LUMO$_{full}$ energy distances and differences Δ with respect to C_{60}

Compound	SOMO–LUMO gap/eV[a]			Δ[b]/eV		
	CV$_{DMF}$	CV$_{DCM}$	MM	CV$_{DMF}$	CV$_{DCM}$	MM
C_{60}	2.05	1.66	2.73	–	–	–
1	1.84	1.49	2.40	0.21	0.17	0.33
2	1.86	1.45	2.32	0.19	0.21	0.41
3	1.86	1.45	2.57	0.19	0.21	0.16
4	1.86	1.50	2.57	0.19	0.16	0.16

[a] SOMO$^{LCOO\bullet}$ = −6.22 eV [32]; LUMO values taken from CV experiments in corresponding solvent and from MM calculations
[b] Δ = (SOMO–LUMO^{C60}) − (SOMO–LUMO^{Fullerosteroid})

functionalized C_{60}. Using the data of the LUMO energies obtained by MM calculations afforded the SOMO–LUMO gap of 2.73 eV for C_{60} and 160–410 meV (∼15–40 kJ/mol) smaller difference for fullerosteroids **1–4** (Table 5). Consequently, it could be supposed that the energy gain obtained by an intermediate formation played more important role in the expression of radical quenching activity in comparison to compound's reducibility.

Morphology

The supramolecular self-assembly of fullerosteroidal conjugates **1–4**, prepared under different conditions, was studied by scanning electron microscopy (SEM). Representative images of samples obtained by slow evaporation of a dilute solution on silicon and brass wafers at room temperature and solid compounds on brass substrate are given in Fig. 7. An influence of the medium polarity on the assembly process in solution was examined using PhMe, CHCl$_3$, and MeOH as well as their different combinations. In all individual solvents low level of self-organization was observed, while the well-organized structures were obtained in the solvent mixtures. Therefore, the size and morphology of the self-organized fullerosteroidal conjugates **1–4** formed in the PhMe/MeOH (5/1, v/v) and more polar CHCl$_3$/PhMe/MeOH (10/5/1, v/v) mixture were investigated. It was also identified that the substrate exerted no appreciable effect on the samples' morphology although the quality of commonly used brass and silicon pads was quite different.

The SEM images presented in Fig. 7 revealed that all studied compounds self-assembled into similar spherical or circular entities with nano- and microscopic dimensions and significant morphological uniformity in both solvent mixtures used. The morphology of the assemblies showed to be non-dependent on the sample concentration (Fig. 73b, 4b). In a less-polar medium on the silicon surface, all compounds formed ordered highly uniform self-
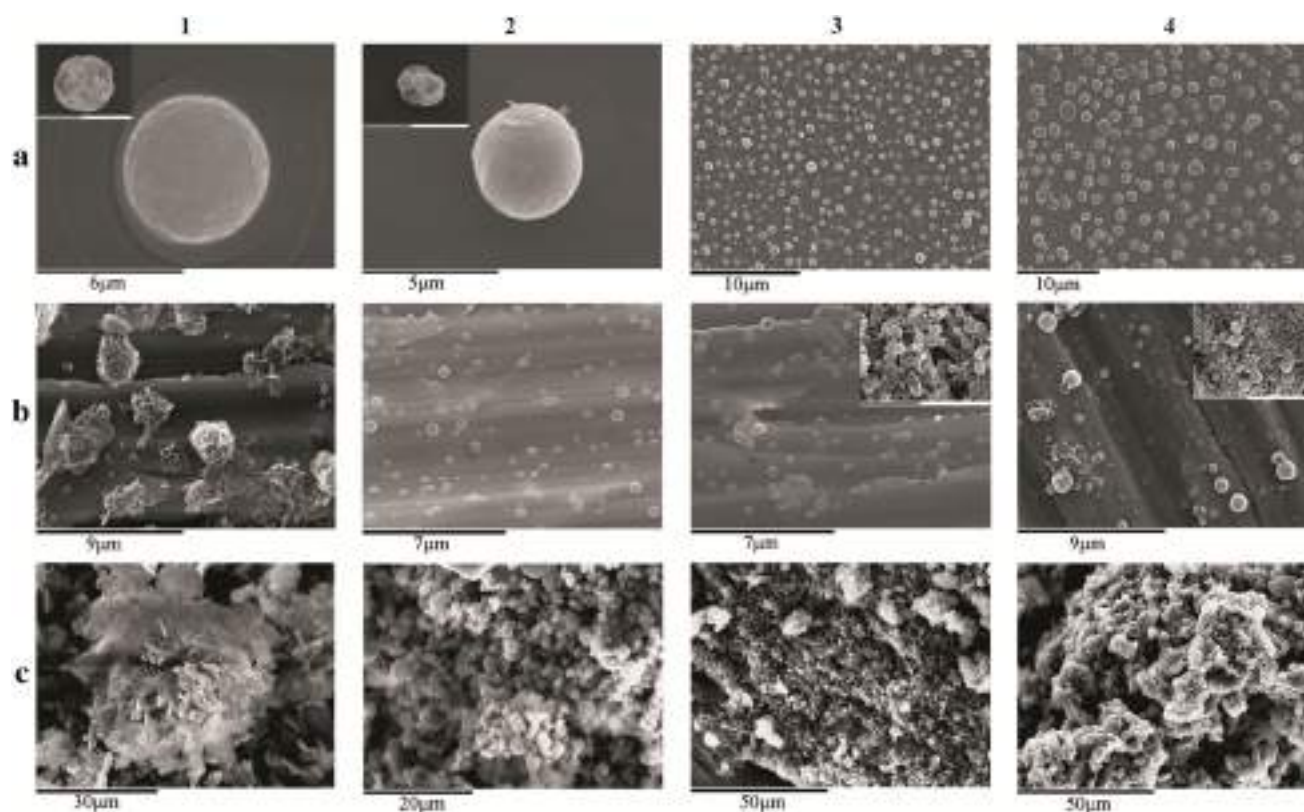
Fig. 7 SEM images of the self-organized particles of fullero-steroid conjugates **1–4** prepared from **a** PhMe/MeOH (5/1) on Si grid; **b** CHCl₃/PhMe/MeOH (10/5/1) on brass substrate, obtained upon slow evaporation of solvent system at room temperature; **c** the solids obtained by precipitation with MeOH deposited on brass substrate. The images of samples prepared from more concentrated solution were shown in insets *3b* and *4b*. The *scale marks* in insets correspond to the same value presented in the large image

aggregates. The fullero-pregnenolone derivatives **1** and **2** assembled into circular particles with ragged surface, implying their layered structure (Fig. 7, insets on 1a and 2a) while fullero-estradiol conjugates **3** and **4** gave smooth round aggregates. It was observed that compounds **1** and **2** formed slightly bigger particles than corresponding derivatives **3** and **4** with diameter of ∼5 and ∼0.2–2 μm, respectively. No other shapes were detected under applied conditions. In more polar medium (CHCl₃/PhMe/MeOH 10/5/1, v/v) compound **1** self-assembled into rose-like micrometer-sized particles (∼3 μm). Obtained architecture resulted from hierarchical self-assembling of initially formed nanometer-sized discoid petal-like components (Fig. 71b). All other fullerosteroidal derivatives gave round uniformly distributed assemblies of about 100–900 nm in diameter (Fig. 72b–4b). The comparison of the results obtained in media of different polarity showed that the aggregates of compounds **2**, **3**, and **4** in both solvent mixtures were uniformly distributed in shape with only variation in size from 100 nm to 5 μm (Fig. 72–4a, b). The self-assembly process in derivative **2** appeared to be the result of the organization of initially formed nanometer-sized disks to hierarchically ordered layered microparticles.

The growth of particles, particularly those of compound **2**, was facilitated in less-polar binary solvent mixture PhMe/MeOH 5/1.

The solid samples formed less-organized aggregates in comparison with those resulted from slow evaporation of the solvent. Their SEM images (Fig. 71–4c) revealed irregularly organized very large spherical particles (up to 400 μm in diameter). In the pregnenolone-appended fullero, derivatives **1** and **2** dispersed leaf-like discoid subunits were observed, while fullero-estradiol conjugates **3** and **4** built spherical cauliflower-like assemblies with no hierarchical architecture.

Conclusions

The additional electrochemical, morphological, and theoretical studies of four fullerosteroidal esters provided better understanding of their properties, giving at the same time a deeper insight into previously observed antioxidant activity. Extensive electrochemical investigations, supported by theoretical calculations showed that the energy gain obtained by formation of the intermediate fullerene-oxidant

species affected the electron-quenching capacity in a greater extent than the reducibility of fullerene subunit. Also, increased polarizability, polarity, lipophilicity, and solvent–solute interactions, achieved by fullerene functionalization, could contribute to the augmentation of the expressed activity. In addition, the tuning of solvent supported self-aggregation was attained by the medium electron-accepting and -donating capacity. In conclusion, presented work could open a possibility to design a broad spectrum of targeted fullerene-based antioxidants.

Experimental

Compounds **1–4** were prepared according to the literature procedure [16]. Their IR, UV, ^{1}H and ^{13}C NMR spectra were identical to the literature data [16]. The solvents used for the cyclic voltammetry and scanning electron microscopy experiments (HPLC grade) were stored over 3Å molecular sieves and degassed under vacuum prior to the use. Ferrocene and TBAP were purchased from Sigma-Aldrich and used as received. For the PCC calculations, the pairwise method was employed for missing values, confidence level 99 %, $p < 0.01$.

Cyclic voltammetry

The electrochemical behavior of fullerosteroids was investigated using 1-mM solution of compounds **1–4** in dry dichloromethane or dimethylformamide containing 0.1-M TBAP as supporting electrolyte. In order to remove oxygen from the electrolyte, the system was bubbled with argon prior to each experiment and the gas inlet left above the liquid surface during the scans. The electrochemical measurements were carried out on CHI760b Electrochemical Workstation potentiostat (CH Instruments, Austin, TX, USA) using a conventional three-electrode cell (1 cm^3) equipped with pre-polished platinum, a Ag/Ag$^+$ electrode (a silver wire in contact with 0.01-M AgNO$_3$ and 0.10-M TBAP in acetonitrile) and the platinum wire as the working, reference and, auxiliary electrodes, respectively, calibrated with ferrocene/ferrocenyl couple (Fc/Fc$^+$) as an internal standard. All experiments were performed at room temperature in the potential range of -2.0 to 0.5 V vs. saturated calomel electrode (SCE), at sweep rates between 0.01 and 1 V cm^{-1}.

SEM

The solid samples were prepared by precipitation from a CHCl$_3$ solution with MeOH and subsequent drying under vacuum. A small amount of each compound was sprinkled on brass substrate. The samples designed for investigation of the size and morphology of self-organized structures formed in solution were prepared at room temperature by "drop drying" method [33]. Briefly, 10 or 50 mm^3 of 0.1-mM solution of fullerosteroids **1–4** in PhMe/MeOH (5/1, v/v) or CHCl$_3$/PhMe/MeOH (10/5/1) was deposited on the substrate surface (10 × 10 mm Si or brass wafer) and left overnight to slowly evaporate in a glass Petri dish under 2 cm^3 of PhMe at room temperature. All samples were gold sputtered in a JFC 1100 ion sputterer and then subjected to SEM observations on a JEOL JSM-840A microscope at an acceleration voltage of 30 kV.

Molecular modeling

All molecules were built in Maestro interface of Schrödinger Suite 2010 (Maestro, version 9.1, Schrödinger, LLC, New York, NY, USA, 2010). In order to better understand spatial properties and behavior of examined molecules, we started Conformational Search from MacroModel module in Schrödinger Suite 2010 (MacroModel, version 9.8, Schrödinger, LLC, New York, NY, USA, 2010). OPLS_2005 force field with water as a solvent and mixed MCMM/low-mode conformational search method [34] were used for that purpose. Every conformation was minimized using Polak–Ribiere conjugate gradient method [35] with maximum of 500 iterations or 0.05 convergence threshold. Duplicates were removed and all structures within energy window of 21 kJ/mol were saved. The most stable structures were used for further calculations. Calculation of molecular descriptors was performed using QikProp module from Schrödinger Suite 2010 (QikProp, version 3.3, Schrödinger, LLC, New York, NY, USA, 2010). For calculation and visualization of electrostatic potential, average ionization potential and HOMO/LUMO orbitals we used single-point DFT B3LYP quantum mechanical calculation with 6-31 + G(d) basis set from Jaguar (Jaguar, version 7.7, Schrödinger, LLC, New York, NY, USA 2010).

References

1. Ali SS, Hardt JI, Quick KL, Sook Kim-Han J, Erlanger BF, Huang TT, Epstein CJ, Dugan LL (2004) Free Radical Biol Med 37:1191
2. Magoulas GE, Garnelis T, Athanassopoulos CM, Papaioannou D, Mattheolabakis G, Avgoustakis K, Hadjipavlou-Litina D (2012) Tetrahedron 68:7041
3. Liu GF, Filipović M, Ivanović-Burmazović I, Beuerle F, Witte P, Hirsch A (2008) Angew Chem Int Ed 47:3991

4. Witte P, Beuerle F, Hartnagel U, Lebovitz R, Savouchkina A, Sali S, Guldi D, Chronakis N, Hirsch A (2007) Org Biomol Chem 5:3599
5. Ali SS, Hardt JI, Dugan LL (2008) Nanomed Nanotechnol 4:283
6. Osuna S, Swart M, Sola M (2010) Chem Eur J 16:3207
7. Hotze EM, Bottero J-Y, Wiesner MR (2010) Langmuir 26:11170
8. Hotze EM, Labille J, Alvarez P, Wiesner MR (2008) Environ Sci Technol 42:4175
9. Geng J, Zhou W, Skelton P, Yue W, Kinloch IA, Windle AH, Johnson BFG (2008) J Am Chem Soc 130:2527
10. Brough P, Bonifazi D, Prato M (2006) Tetrahedron 62:2110
11. Liu H, Li Y, Jiang L, Luo H, Xiao S, Fang H, Li H, Zhu D, Yu D, Xu J, Xiang B (2002) J Am Chem Soc 124:13370
12. Sathish M, Miyazawa K (2007) J Am Chem Soc 129:13816
13. Prassides K, Keshavarz-K M, Beer E, Bellavia C, González R, Murata Y, Wudl F, Cheetham AK, Zhang JP (1996) Chem Mater 8:2405
14. Wang N, Li Y, He X, Gan H, Li Y, Huang C, Xu X, Xiao J, Wang S, Liu H, Zhu D (2006) Tetrahedron 62:1216
15. Cassell AM, Asplund CL, Tour JM (1999) Angew Chem Int Ed 38:2403
16. Bjelaković M, Godjevac D, Milić D (2007) Carbon 45:2260
17. Hummelen JC, Knight BW, LePeq F, Wudl F (1995) J Org Chem 60:532
18. Schuster DI (2000) Carbon 38:1607
19. MacMahon S, Fong R II, Baran PS, Safonov I, Wilson SR, Schuster DI (2001) J Org Chem 66:5449
20. Li L-S, Hu Y-J, Wu Y, Wu Y-L, Yue J, Yang F (2001) J Chem Soc Perkin Trans 1:617
21. Ishi-I T, Shinkai S (1999) Tetrahedron 55:12515
22. Chuard T, Deschenaux R (2002) J Mater Chem 12:1944
23. Maggini M, Guldi DM, Mondini S, Scorrano G, Paolucci F, Ceroni P, Roffia S (1998) Chem Eur J 4:1992
24. Dubois D, Moninot G, Kutner W, Jones MT, Kadish KM (1992) J Phys Chem 96:7137
25. Allemand PM, Koch A, Wudl F, Rubin Y, Diederich F, Alvarez MM, Anz SJ, Whetten RL (1991) J Am Chem Soc 113:1050
26. Gritzner G, Kuta J (1984) Pure Appl Chem 56:461
27. Evans DH, Gilicinski AG (1992) J Phys Chem 92:2528
28. Cardona CM, Li W, Kaifer AE, Stockdale D, Bazan GC (2011) Adv Mat 23:2367
29. Hansen WN, Hansen GJ (1987) Phys Rev A 36:1396
30. Hirsch A, Brettreich M (2005) Fullerenes: chemistry and reactions. Wiley, Weinheim, p 35
31. NCSS 8 Software Package, free trial version. Available at www.ncss.com
32. Matsubayashi K, Goto T, Togaya K, Kokubo K, Oshima T (2008) Nanoscale Res Lett 3:237
33. Babu SS, Möhwald H, Nakanishi T (2010) Chem Soc Rev 39:4021
34. Kolossváry I, Guida WC (1999) J Comput Chem 20:1671
35. Polak E, Ribiere G (1969) Rev Fr Inform Rech O Serie Rouge 3:35